

Supplementary

Thiosemicarbazone derivatives of nickel and copper: the unprecedented coordination of furan ring in octahedral nickel(II) and of triphenylphosphine in three-coordinate copper(I) complexes

Tarlok Singh Lobana,^{a*} Poonam Kumari,^a Rekha Sharma,^a Alfonso Castineiras,^b Ray Jay Butcher,^c Takashiro Akitsu,^d Yoshikazu Aritake^d

^a *Department of Chemistry, Guru Nanak Dev University, Amritsar –143 005, India*

^b *Departamento De Química Inorganica, Facultad de Farmacia, Universidad de Santiago, 15782-Santiago, Spain*

^c *Department of Chemistry, Howard University, Washington DC 20059, USA*

^d *Department of Chemistry, Tokyo University of Science, Tokyo –1628601, Japan*

* To whom correspondence should be addressed. E-mail: tarlokslobana@yahoo.co.in. (T. S. L.); Fax +91-183-2-258820

Spectroscopy (IR, NMR, UV-vis)

The ligands show IR bands due to $\nu(\text{N}^1\text{-H})$ and $\nu(\text{N}^2\text{-H})$ moieties in the region, 3459–3206 cm^{-1} . In their respective complexes **1–8**, bands due to $\nu(\text{N}^1\text{-H})$ appears in the the range, 3408–3357 cm^{-1} . The $\nu(\text{N}^2\text{-H})$ bands appear at 3129 and 3119 cm^{-1} in complexes **7** and **8** while this band disappear in complexes **1–6**. This reveals that the ligands are coordinated to the metal center in the anionic form in complexes **1–6** and in neutral form in complexes **7** and **8**. The diagnostic $\nu(\text{C-S})$ bands lie in the range, 713–752 cm^{-1} in the complexes **1–6** and $\nu(\text{C=S})$ band at 848 and 795 cm^{-1} in complexes **7** and **8** respectively (cf. free ligands, 819–739 cm^{-1}). Other characteristic bands are given in the experimental section.

Free ligands (HaftscN-R^2 , HattscN-R^2 ; $\text{R}^2 = \text{Me, Et, Ph}$) show a signal at low field (8.56–9.40 ppm) due to the presence of hydrazinic proton ($-\text{N}^2\text{H}-$). This signal appears at δ 11.42 and 11.30 ppm in complexes **7** and **8** respectively, which shows a downfield shift vis-à-vis free ligands which confirmed that thio- ligands are coordinating to Cu in neutral form. Further, the ^{31}P NMR spectra of complexes **7** and **8** showed one signal at δ 31.2 and 30.8 ppm respectively, with a coordination shift of $\Delta\delta$ 35.8 (**7**) and 35.4 (**8**) ppm. However this signal is absent in the spectra of complexes **3–6**, thus confirming

deprotonation of these ligands in their respective complexes. Complexes **1–3** are paramagnetic, so their NMR spectra were recorded by opening the window from +100 to -100 ppm. In these complexes, signals show downfield shift relative to their respective ligands, except N¹H signal (-4.09, **1**; -3.01, **2**; -1.12 ppm, **3**). In complexes **4–8**, signals are well resolved and are given in the experimental section.

In the O, N, S- donor ligand, HaftscN-Me, intense absorption bands at 207, 220 and 314 nm are assigned to $\pi \rightarrow \pi^*$ and $n \rightarrow \pi^*$ transitions respectively. These bands in complex **1** appear at 247 and 301 nm. Two bands at 331 and 406 nm are assigned to S \rightarrow Ni charge transfer transitions, while the bands at 671 and 982 nm are assigned to the d-d transitions: ${}^3A_{2g}(F) \rightarrow {}^3T_{1g}(P)$ and ${}^3A_{2g}(F) \rightarrow {}^3T_{1g}(F)$ respectively. The various transitions in complexes **2** and **3** are assigned as follows: $\pi \rightarrow \pi^*$ (248, **2**; 247, **3**), $n \rightarrow \pi^*$ (301, **2**; 301, **3**), S \rightarrow Ni(CT) (331, 405, **2**; 330, 408 **3**), ${}^3A_{2g}(F) \rightarrow {}^3T_{1g}(P)$ (675, **2**; 681, **3**) and ${}^3A_{2g}(F) \rightarrow {}^3T_{1g}(F)$ (983, **2**; 985, **3**) (Table 1). Similarly, in the N, S- donor ligand, HattscN-Me, the $\pi \rightarrow \pi^*$ (213, 257 nm) shift to 229 nm in square planar complex **4**. The $n \rightarrow \pi^*$ transition (320 nm in ligand) merges with LMCT (S \rightarrow Ni) + ν_3 (d-d) transitions and appears as an intense band at 337 nm. A band at 412 nm, attributed to ${}^1A_{1g} \rightarrow {}^1A_{2g}$ transition, appears as shoulder to main band. Complexes **5** and **6**, have shown similar transitions in the ranges : 212–269 ($\pi \rightarrow \pi^*$), 343 ($n \rightarrow \pi^*$, S \rightarrow Ni + ${}^1A_{1g} \rightarrow {}^1E_g$) and 410–415 nm (${}^1A_{1g} \rightarrow {}^1A_{2g}$) (Table 2).

IR spectra of the ligands

HaftscN-Me: IR (KBr, cm^{-1} , selected absorption bands): 3445br ($\nu(\text{N}^1\text{-H})$); 3241s ($\nu(\text{N}^2\text{-H})$); 3051w, 2984w ($\nu(\text{C-H})$); 1555s, 1496s ($\nu(\text{C=N}) + \nu(\text{C=C})$); 1077s, 1047s ($\nu(\text{C-N})$); 739s ($\nu(\text{C-S})$).

HaftscN-Et: IR (KBr, cm^{-1} , selected absorption bands): 3334br ($\nu(\text{N}^1\text{-H})$); 3272br ($\nu(\text{N}^2\text{-H})$); 2977w, 2940w, 2866w ($\nu(\text{C-H})$); 1539s, 1517s ($\nu(\text{C=N}) + \nu(\text{C=C})$); $\nu(\text{C-N})$; 744s ($\nu(\text{C-S})$).

HaftscN-Ph: IR (KBr, cm^{-1} , selected absorption bands): 3459s ($\nu(\text{N}^1\text{-H})$); 3341s ($\nu(\text{N}^2\text{-H})$); 3155w, 3103w, 2835w ($\nu(\text{C-H})$); 1558s, 1526s ($\nu(\text{C=N}) + \nu(\text{C=C})$); 1068s, 1018s, 934s ($\nu(\text{C-N})$); 757s ($\nu(\text{C-S})$).

HattscN-Me: IR (KBr, cm^{-1} , selected absorption bands): 3446br ($\nu(\text{N}^1\text{-H})$); 3385s ($\nu(\text{N}^2\text{-H})$); 2989w, 2931w ($\nu(\text{C-H})$); 1558s, 1542s ($\nu(\text{C=N}) + \nu(\text{C=C})$); 1053s, 1035s, 959s ($\nu(\text{C-N})$); 819s ($\nu(\text{C-S})$).

HattscN-Et: IR (KBr, cm^{-1} , selected absorption bands): 3358br ($\nu(\text{N}^1\text{-H})$); 3206s ($\nu(\text{N}^2\text{-H})$); 3128w, 2962w, 2882w ($\nu(\text{C-H})$); 1596s, 1517s ($\nu(\text{C=N}) + \nu(\text{C=C})$); 1096s, 1053s, 967s ($\nu(\text{C-N})$); 811s ($\nu(\text{C-S})$).

HattscN-Ph: IR (KBr, cm^{-1} , selected absorption bands): 3390br ($\nu(\text{N}^1\text{-H})$); 3248s ($\nu(\text{N}^2\text{-H})$); 3052w, 2906w ($\nu(\text{C-H})$); 1587s, 1531s ($\nu(\text{C=N}) + \nu(\text{C=C})$); 1047s, 1027s ($\nu(\text{C-N})$); 817s ($\nu(\text{C-S})$).

^1H NMR spectra of ligands: **HattscN-Me,** ^1H NMR (δ , CDCl_3): δ 8.62 (1H, s, N^2H), 7.66 (1H, s, br, N^1H), 7.48 (1H, dd, C^6H), 6.73 (1H, dd, C^4H), 6.47 (1H, q, C^5H), 3.25 (3H, t, $\text{CH}_3(\text{C}^2)$), 2.21 (3H, d, $\text{CH}_3(\text{N}^1)$) ppm. **HattscN-Et,** ^1H NMR (δ , CDCl_3): δ 8.56 (1H, s, N^2H), 7.66 (1H, s, br, N^1H), 7.59 (1H, d, C^6H), 6.72 (1H, s, C^4H), 6.47 (1H, dd, C^5H), 3.72 (2H, m, CH_2), 2.20 (3H, d, $\text{CH}_3(\text{C}^2)$), 1.69 (s, 3H, $\text{CH}_3(\text{N}^1)$) ppm. **HattscN-Ph,** ^1H NMR (δ , CDCl_3): δ 9.40 (1H, s, N^2H), 8.71 (1H, s, N^1H), 7.69 (2H, m, *o*-H(Ph)), 7.52 (1H, dd, *p*-H(Ph)), 7.40 (1H, m, *m*-H(Ph)), 7.24 (2H, dd, C^6H), 6.79 (1H, dd, C^4H), 6.54 (1H, dd, C^5H), 2.35 (3H, s, $\text{CH}_3(\text{C}^2)$) ppm. **HattscN-Me,** ^1H NMR (δ , CDCl_3): δ 8.59 (1H, s, N^2H), 7.52 (1H, s, br, N^1H), 7.34 (1H, dd, C^6H), 7.29 (1H, dd, C^4H), 7.03 (1H, q, C^5H), 3.27 (3H, t, $\text{CH}_3(\text{C}^2)$), 2.28 (3H, d, $\text{CH}_3(\text{N}^1)$) ppm. **HattscN-Et,** ^1H NMR (δ , CDCl_3): δ 8.56 (1H, s, N^2H), 7.47 (1H, s, br, N^1H), 7.33 (1H, dd, C^6H), 7.29 (1H, m, C^4H), 7.03 (1H, m, C^5H), 3.76 (2H, m, CH_2), 2.25 (3H, d, $\text{CH}_3(\text{C}^2)$), 1.34 (3H, s, $\text{CH}_3(\text{N}^1)$) ppm. **HattscN-Ph,** ^1H NMR (δ , CDCl_3): δ 9.30 (1H, s, N^2H), 8.69 (1H, s, N^1H), 7.71 (1H, d, C^6H), 7.69 ((1H, d, C^4H), 7.39 (3H, m, *o*-H+ *p*-H(Ph)), 7.23 (1H, t, *m*-H(Ph)), 7.06 (1H, q, C^5H), 2.31 (3H, d, $\text{CH}_3(\text{C}^2)$) ppm.

Table 1. Electronic spectral data: $\lambda_{\max/\text{nm}}$ (ϵ /L mol⁻¹ cm⁻¹)^a

Compound	$\pi \rightarrow \pi^*$	$n \rightarrow \pi^*$	LMCT(S \rightarrow Ni)	d-d
[Ni(aftscN-Me) ₂] ^a 1	247(19520)	301(20980)	331(19940)	671 (510)
			406(23680)	982 (540)
[Ni(aftscN-Et) ₂] ^a 2	248(19430)	301(20950)	331(19930)	675 (380)
			405 (23730)	983 (410)
[Ni(aftscN-Ph) ₂] ^a 3	247(19410)	301(21000)	330 (19950)	681(360)
			408 (23810)	985(400)

^a 10⁻⁴M in CH₃OH

HaftscN-Me^a: 207(7080), 220 (4500) $\pi \rightarrow \pi^*$, 314(18540) $n \rightarrow \pi^*$

HaftscN-Et^a: 208(7310), 233 (4340) $\pi \rightarrow \pi^*$, 314(18100) $n \rightarrow \pi^*$

HaftscN-Ph^a: 209(11140), 240 (7500) $\pi \rightarrow \pi^*$, 320(18570) $n \rightarrow \pi^*$

Table 2. Electronic spectral data: $\lambda_{\max/\text{nm}}$ (ϵ /L mol⁻¹ cm⁻¹)^a

Compound	$\pi \rightarrow \pi^*$	$n \rightarrow \pi^*$ + LMCT (S \rightarrow Ni) + ν_3 (d-d)	ν_2 (d-d)
[Ni(attscN-Me) ₂] ^a 4	229(10970)	337(12750)	412 (4000)
	270 (11000)		
[Ni(attscN-Et) ₂] ^a 5	231(11800)	343(14080)	410 (4000)
	269(12550)		
[Ni(attscN-Ph) ₂] ^a 6	212 (15010)	343(18940)	415 (5200)
	264 (22820)		

^a 10⁻⁴M in CH₃OH,

HattscN-Me^a: 213(12050), 257(10020) sh $\pi \rightarrow \pi^*$, 320(24530) $n \rightarrow \pi^*$

HattscN-Et^a: 212(3990), 260 sh(3590) $\pi \rightarrow \pi^*$, 328(8990) $n \rightarrow \pi^*$

HattscN-Ph^b: 268 sh (8210) $\pi \rightarrow \pi^*$, 336(8210) $n \rightarrow \pi^*$

^b 10⁻⁴ M in DMSO

Melting Points of complexes: m. p. 220-222 °C (**1**), 228-230 °C (**2**), 234-236 °C (**3**), 215-216 °C (**4**), 210-212 °C (**5**), 155-160 °C (**6**)

Crystal structure

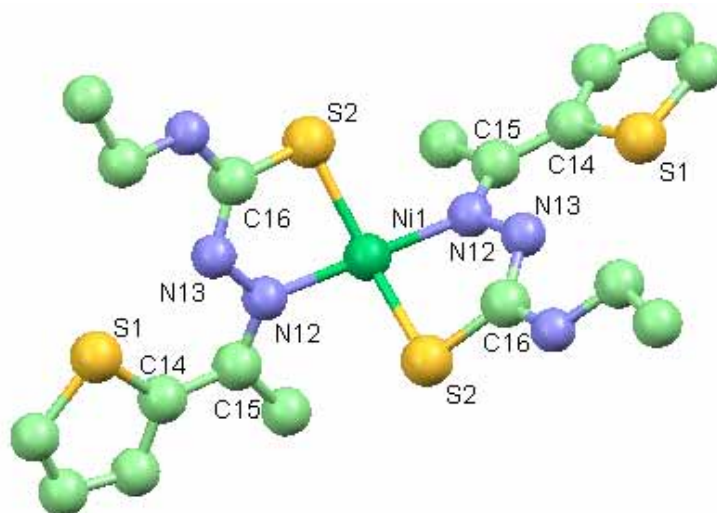


Fig. 1 Molecular structure of complex $[\text{Ni}(\text{attsN-Et})_2]$ **5**

Packing Interactions

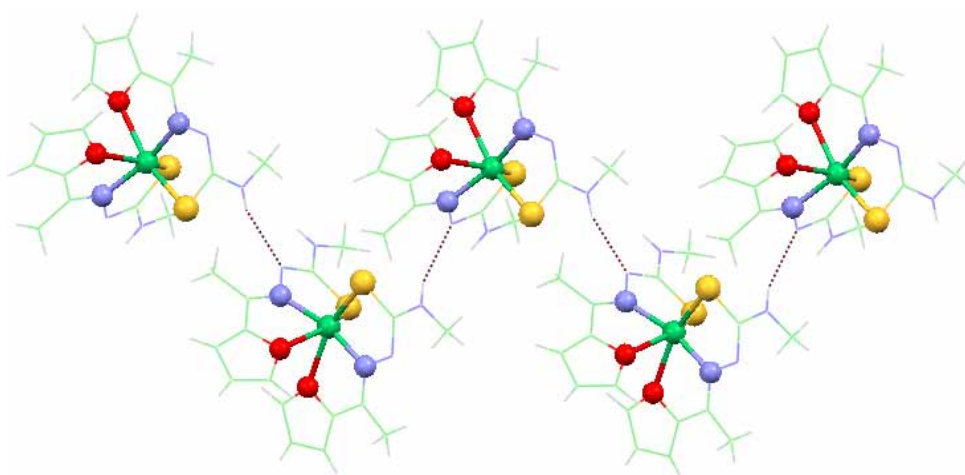


Fig. 2 Packing diagram of complex **1**, showing interaction, $\{\text{N}^2 \cdots \text{H}(\text{N}^1), 2.33 \text{ \AA}\}$ in 1D chain

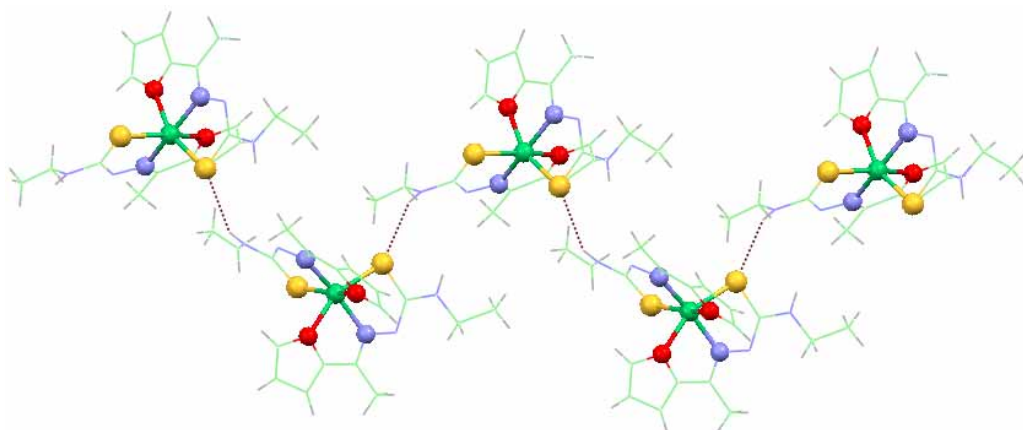


Fig. 3 Packing diagram of complex **2**, showing interaction, {C-S \cdots H(N¹), 2.73 Å} in 1D chain

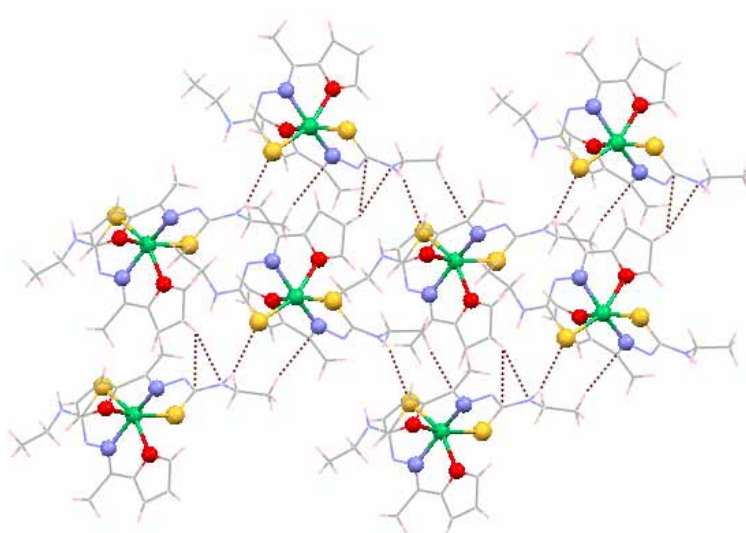


Fig. 4 Packing diagram of complex **2**, showing 2D network

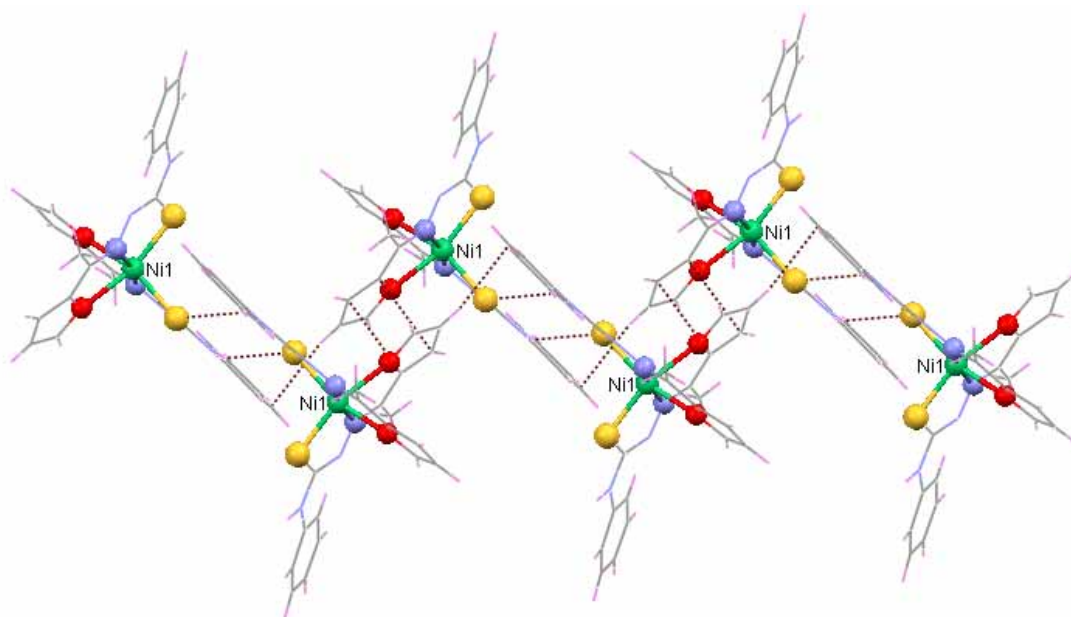


Fig. 5 Packing interactions in **3**, showing intermolecular interactions of type 1 molecules, {C-S...HN¹, 2.734, (furan)C-H...π(ph), 2.837, (furan)π...π(furan) 3.318 Å} in 1D chain

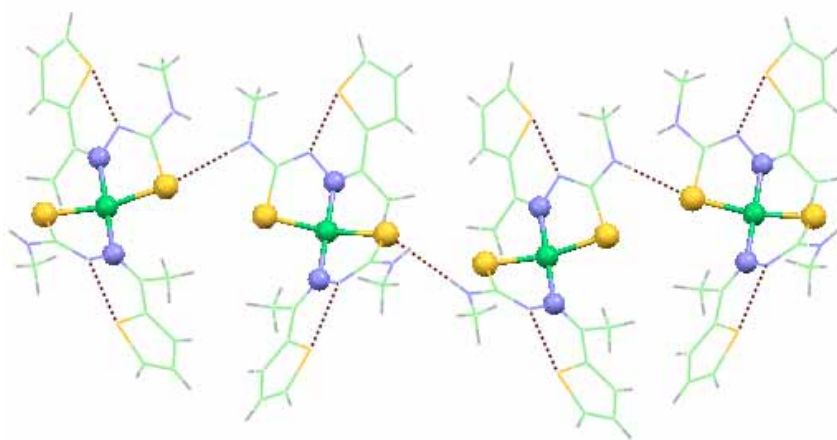


Fig. 6 Packing diagram of complex **4**, showing intramolecular, {C₄H₃S...N², 2.63 Å} and intermolecular interactions, {C-S...HN¹, 2.73 Å} in 1D chain

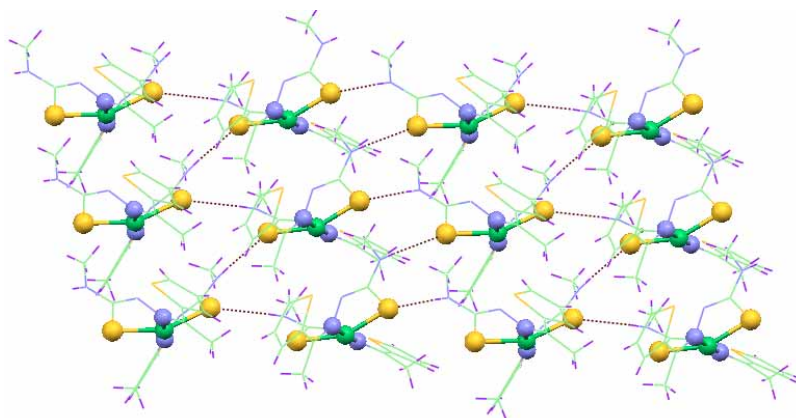


Fig. 7 Packing diagram of complex **4** showing 2D network

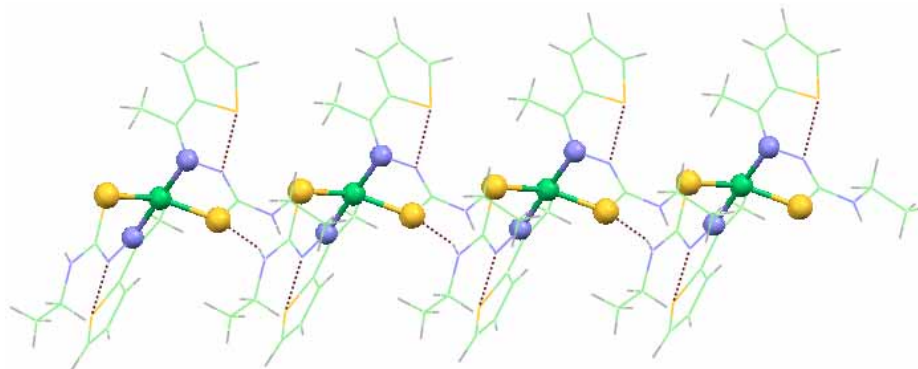


Fig. 8 Packing diagram of complex **5**, showing intramolecular, $\{C_4H_3S \cdots N^2, 2.65 \text{ \AA}\}$ and intermolecular interactions, $\{C-S \cdots HN^1, 2.82 \text{ \AA}\}$ in 1D chain

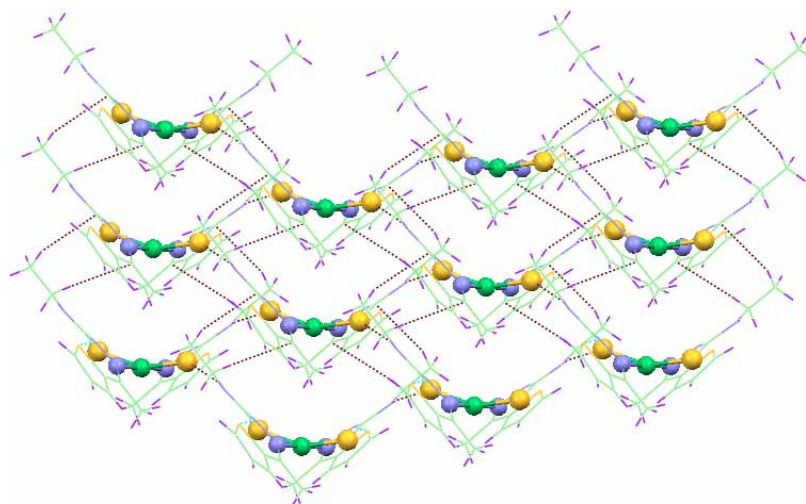


Fig. 9 Packing diagram of complex **5**, showing 2D network

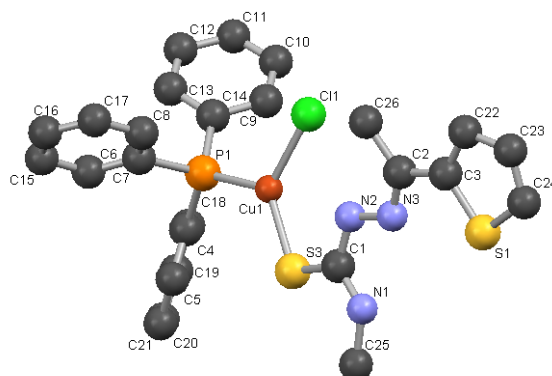


Fig. 10 Molecular structure of complex $[\text{CuCl}(\eta^1\text{-S-HattscN-Me})(\text{Ph}_3\text{P})]$ **8**

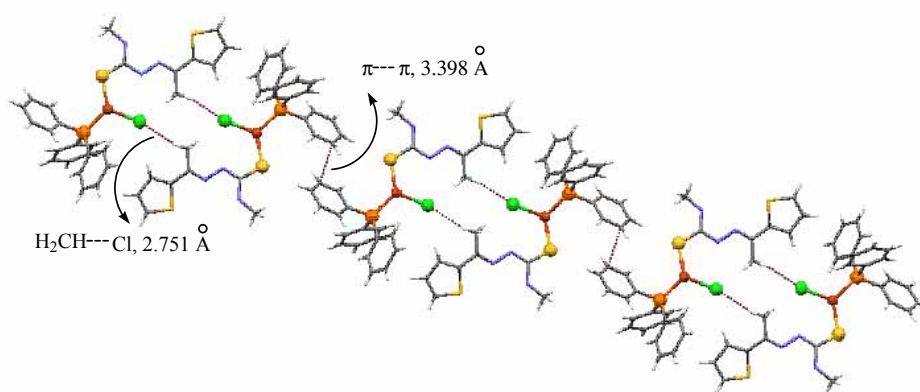
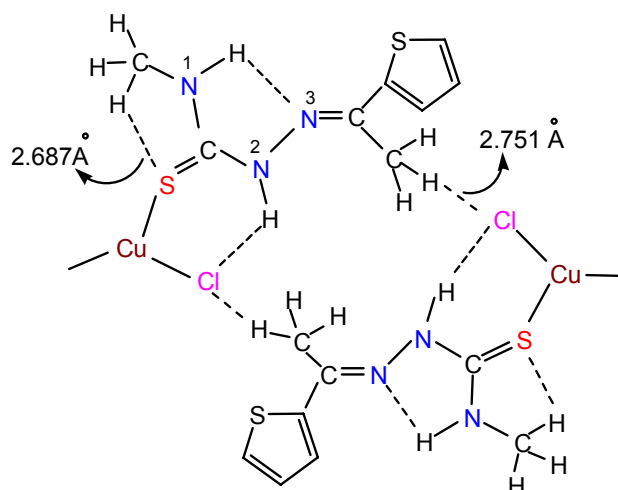


Fig. 11 Packing diagram of complex **8**



Scheme 1. Various intra- and inter-molecular interactions of $[\text{CuCl}(\eta^1\text{-S-HattscN-Me})(\text{Ph}_3\text{P})]$ **8**

Table 3. (C² methyl)C-H···H-C(furan) interactions in ligand (Haftsc-N-Me) according to our Chem. Draw Schemes are given below according to their X-ray structures of complexes (1–3)

Haftsc-N-Me	2.110 Å (C ⁴ -H···H-C ⁶)
1	2.513 Å (C ²⁸ -H···H-C ²³), 2.390 Å (C ¹⁸ -H···H-C ¹³)
2	2.538 Å (C ²⁰ -H···H-C ¹⁴), 2.457 Å (C ³⁰ -H···H-C ²⁴), 2.559 Å (C ⁴⁰ -H···H-C ³⁴), 2.391 Å (C ⁵⁰ -H···H-C ⁴⁴)
3	2.342 Å (C ¹⁵⁰ -H···H-C ¹³), 2.430 Å (C ²⁵⁰ -H···H-C ²³), 2.450 Å (C ³⁵⁰ -H···H-C ³³)

Table 4. Hydrogen Bonds (Å)

Complex 1			
N ² ···H-N ¹	2.33		
(furan)C-H···S-C	2.85	(furan)C-H···N ²	2.58
Complex 2			
C-S···H-N ¹	2.73		
(furan)C-H···S-C	2.81	(furan)C-H···N ¹	2.72
Complex 3			
C-S···H-N ¹	2.73	(furan)C-H···□(ph)	2.84
(furan)□···□(furan)	3.32	(furan)C-H···□(ph)	3.00
H-N ¹ ···HCH ₂ (C ²)	2.62	C-S···HCH ₂ (C ²)	2.83
(Ph)C-H···□(ph)	2.86	(ph)C-H···N ²	2.66
C-S···HN ¹	2.66		
Complex 4			
S···N ²	2.63	C-S···H(N ¹)	2.73
Complex 5			
S···N ²	2.65	C-S···H(N ¹)	2.82
C ² ···HCH(N ¹)	2.85	C-S···HCH ₂ CH ₂ (N ¹)	2.83

Table 5. Selected bond lengths (Å) and bond angles (°) of complexes 1–5, 7 and 8

Complex 1			
Ni(1)-N(12)	2.016(12)	Ni(1)-S(1)	2.313(4)
Ni(1)-O(11)	2.358(11)	Ni(1)-N(22)	2.018(12)
Ni(1)-S(2)	2.313(4)	Ni(1)-O(21)	2.319(10)
C(16)-S(1)	1.738(15)	C(26)-S(2)	1.748(16)
C(15)-N(12)	1.299(19)	C(25)-N(22)	1.305(19)
O(21)-Ni(1)-N(22)	74.70(4)	N(22)-Ni(1)-S(2)	83.79(4)
S(1)-Ni(1)-N(12)	83.52(4)	N(12)-Ni(1)-O(11)	74.30(4)

O(21)-Ni(1)-O(11)	73.26(4)	S(2)-Ni(1)-S(1)	100.71(15)
N(22)-Ni(1)-N(12)	162.01(5)	O(21)-Ni(1)-S(2)	158.04(3)
O(11)-Ni(1)-S(1)	150.94(3)		
Complex 2			
One independent molecule			
Ni(1)-N(12)	2.032(3)	Ni(1)-S(1)	2.3109(10)
Ni(1)-O(11)	2.284(3)	Ni(1)-N(22)	1.990(3)
Ni(1)-S(2)	2.2902(11)	Ni(1)-O(21)	2.341(3)
C(17)-S(1)	1.736(4)	C(27)-S(2)	1.757(4)
C(16)-N(12)	1.245(4)	C(26)-N(22)	1.346(5)
O(21)-Ni(1)-N(22)	91.37(11)	N(22)-Ni(1)-S(2)	84.00(10)
S(1)-Ni(1)-N(12)	84.56(8)	N(12)-Ni(1)-O(11)	74.97(10)
O(21)-Ni(1)-O(11)	79.89(10)	S(2)-Ni(1)-S(1)	102.21(4)
N(22)-Ni(1)-N(12)	161.99(11)	O(21)-Ni(1)-S(2)	157.54(7)
O(11)-Ni(1)-S(1)	157.78(8)		
Second independent molecule			
Ni(2)-N(32)	2.052(3)	Ni(2)-S(3)	2.3163(10)
Ni(2)-O(31)	2.339(3)	Ni(2)-N(42)	2.028(4)
Ni(2)-S(4)	2.3348(11)	Ni(2)-O(41)	2.202(3)
C(37)-S(3)	1.753(4)	C(47)-S(4)	1.700(4)
C(36)-N(32)	1.306(5)	C(46)-N(42)	1.276(5)
O(31)-Ni(2)-N(32)	75.50(12)	N(32)-Ni(2)-S(3)	84.04(10)
S(4)-Ni(2)-N(42)	83.42(10)	N(42)-Ni(2)-O(41)	75.03(13)
O(41)-Ni(2)-O(31)	79.89(11)	S(3)-Ni(2)-S(4)	101.41(4)
N(42)-Ni(2)-N(32)	160.84(13)	O(41)-Ni(2)-S(4)	157.69(8)
O(31)-Ni(2)-S(3)	157.36(8)		
Complex 3			
One independent molecule			
Ni(1)-N(12)	2.0192(14)	Ni(1)-S(1)	2.3024(5)
Ni(1)-O(11)	2.3525(12)	Ni(1)-N(22)	2.0068(14)
Ni(1)-S(2)	2.3089(5)	Ni(1)-O(21)	2.2588(12)
C(16)-S(1)	1.7346(1)	C(26)-S(2)	1.7497(17)
C(15)-N(12)	1.300(2)	C(25)-N(22)	1.303(2)
O(21)-Ni(1)-N(22)	75.12(5)	N(22)-Ni(1)-S(2)	83.60(4)
S(1)-Ni(1)-N(12)	83.82(4)	N(12)-Ni(1)-O(11)	73.95(5)
O(21)-Ni(1)-O(11)	80.12(4)	S(2)-Ni(1)-S(1)	101.261(18)
N(22)-Ni(1)-N(12)	164.43(6)	O(21)-Ni(1)-S(2)	155.63(4)
S(1)-Ni(1)-O(11)	157.10(3)		
Second independent molecule			
Ni(2)-N(32)	2.0194(14)	Ni(2)-S(3)	2.3105(5)
Ni(2)-O(31)	2.2964(13)	C(36)-S(3)	1.7505(17)

C(35)-N(32)	1.301(2)		
O(31)-Ni(2)-N(32)	75.09(5)	N(32)-Ni(2)-S(3)	83.52(4)
N(32)-Ni(2)-S(3)	83.52(4)	O(31)-Ni(2)-N(32)	86.14(5)
O(31)-Ni(2)-O(31)	77.94(7)	S(3)-Ni(2)-S(3)	100.32(3)
N(32)-Ni(1)-N(32)	155.90(9)	O(31)-Ni(2)-S(3)	157.55(3)
Complex 4			
Ni(1)-N(12)	1.912(2)	Ni(1)-S(1)	2.1950(8)
C(16)-S(1)	1.753(3)	C(15)-N(12)	1.312(4)
N(12)-Ni(1)-S(1)	93.88(7)	N(12)-Ni(1)-S(1)	85.32(8)
N(12)-Ni(1)-N(12)	176.3(2)	S(1)-Ni(1)-S(1)	155.40(6)
Complex 5			
Ni(1)-N(12)	1.898(3)	Ni(1)-S(1)	2.204(9)
C(16)-S(2)	1.737(4)	C(15)-N(12)	1.314(5)
N(12)-Ni(1)-S(2)	94.82(9)	N(12)-Ni(1)-S(2)	84.80(9)
N(12)-Ni(1)-N(12)	178.3(2)	S(1)-Ni(1)-S(2)	154.47(6)
Complex 7			
Cu(1)-S(2)	2.218(11)	Cu(1)-P(1)	2.223(10)
Cu(1)-Br(1)	2.373(6)	S(2)-C(19)	1.721(4)
C(19)-N(2)	1.334(5)	N(2)-N(3)	1.387(4)
S(2)-Cu(1)-P(1)	125.98(4)	S(2)-Cu(1)-Br(1)	122.37(3)
P(1)-Cu(1)-Br(1)	111.53(3)	C(19)-S(2)-Cu(1)	111.44(13)
Complex 8			
Cu(1)-S(3)	2.2244(9)	Cu(1)-P(1)	2.2161(8)
Cu(1)-Cl(1)	2.2373(10)	S(3)-C(1)	1.713(3)
P(1)-Cu(1)-Cl(1)	114.99(4)	S(3)-Cu(1)-Cl(1)	120.27(4)
P(1)-Cu(1)-S(3)	124.61(3)	C(1)-S(3)-Cu(1)	110.69(11)

The single crystal of compound (HaftscN-Me) was mounted on Xcalibur, Ruby, Gemini diffractometer, equipped with a graphite monochromator and Mo-K α radiation ($\lambda = 0.71073 \text{ \AA}$). The unit cell dimensions and intensity data were measured at 123(2) K.

Table 6. Crystallographic data of ligand HaftscN-Me

	HaftscN-Me
Empirical formula	C ₁₆ H ₂₄ N ₆ O ₃ S ₂
M	412.53
T(K)	123(2)
Crystal system	Orthorhombic
Space group	P b c n
a(Å)	13.1262(4)
b(Å)	7.4010(2)
c(Å)	20.7051(5)
α(°)	90.00
β(°)	90.00
γ(°)	90.00
V(Å ³)	2011.43(9)
Z	4
D _{calcd} (g cm ⁻³)	1.362
μ(mm ⁻¹)	0.294
Reflections collected	10754
Independent reflections	3407 [R(int)= 0.0281]
final R indices[I>2σ(I)]	R1= 0.0392, wR2= 0.1061